

# Lateral heterogeneities in supported bilayers from pure and mixed phosphatidylethanolamine demonstrating hydrogen bonding capacity

Matthew R. Nussio and Nicolas H. Voelcker<sup>a),b)</sup>

*School of Chemistry, Physics and Earth Sciences, Flinders University, Sturt Road, Bedford Park, Adelaide, South Australia 5001, Australia*

Matthew J. Sykes

*Department of Clinical Pharmacology, Flinders University, Sturt Road, Bedford Park, Adelaide, South Australia 5001, Australia*

Steven J. P. McInnes, Christopher T. Gibson, and Rachel D. Lowe

*School of Chemistry, Physics and Earth Sciences, Flinders University, Sturt Road, Bedford Park, Adelaide, South Australia 5001, Australia*

John O. Miners

*Department of Clinical Pharmacology, Flinders University, Sturt Road, Bedford Park, Adelaide, South Australia 5001, Australia*

Joseph G. Shapter<sup>a),b)</sup>

*School of Chemistry, Physics and Earth Sciences, Flinders University, Sturt Road, Bedford Park, Adelaide, South Australia 5001, Australia*

(Received 19 September 2008; accepted 6 November 2008; published 2 February 2009)

The phase behavior and lateral organization of saturated phosphatidylethanolamine (PE) and phosphatidylcholine (PC) bilayers were investigated using atomic force microscopy (AFM) and force-volume (FV) imaging for both pure and two component mixed layers. The results demonstrated the existence of unexpected segregated domains in pure PE membranes at temperatures well below the transition temperature ( $T_m$ ) of the component phospholipid. These domains were of low mechanical stability and lacked the capacity for hydrogen bonding between lipid headgroups. Temperature dependent studies for different PC/PE ratios using AFM also demonstrated the mixing of these phospholipid bilayers to exhibit only a single gel to liquid transition temperature. Further work performed using FV imaging and chemically modified probes established that no lipid segregation exists at the PC/PE ratios investigated. © 2008 American Vacuum Society. [DOI: 10.1116/1.3040158]

## I. INTRODUCTION

Synthetic lipid bilayer membranes are used extensively as model systems for the study of membrane organization and physiological function.<sup>1-4</sup> Despite their apparent simplicity, such membranes potentially exhibit complex behavior with respect to phase equilibria and lateral heterogeneity. Understanding these properties is of crucial importance for elucidating the mechanisms by which lipid constituents influence membrane function. Moreover, the involvement of membranes in diverse, critical cellular functions justifies the use of a spectrum of natural phospholipids in synthetic bilayers. Characterization of the spatial distribution of these components in a membrane and their effects on physical properties is key to ultimately understanding multicomponent lipid membranes.

Phosphatidylcholine (PC) and phosphatidylethanolamine (PE) are the main lipids present in the membranes of eukaryotic cells. Although variable between various organelle, the relative abundance and mixing behavior of these phospholip-

ids are of significant interest. PC and PE lipids differ only by their substituents at the N-terminus of the headgroup (Fig. 1). PC contains a bulky quaternary amine with methyl substituents while PE has a primary amine headgroup. Molecular simulation studies have demonstrated the ability of PE to interact strongly with itself and neighboring lipids via inter- and intramolecular hydrogen bonding.<sup>5</sup> This generates a close-packed lipid bilayer with the hydrocarbon tails aligned, decreasing the space occupied by each lipid molecule.<sup>6</sup> Since PC lipids comprise a bulky choline headgroup, and are subjected to dipole-dipole interactions, there exist repulsive forces when the dipoles are aligned parallel to the bilayer normal. This electrostatic repulsion causes the PC lipids to tilt with respect to each other and, in contrast to PE lipids, generates a larger area occupied per lipid molecule. Incorporation of PE lipids in a PC bilayer, however, results in a significant decrease in the area occupied per lipid for PC, since PE can readily form intermolecular hydrogen bonds (attractive interactions) with neighboring PC molecules and relieve the electrostatic repulsion between PC headgroups.<sup>7</sup> Lateral ordering of these mixed systems has been the subject of debate, with studies suggesting either a regular distribution, otherwise known as superlattice formation<sup>8,9</sup> or domain formation.<sup>10,11</sup> Understanding the lateral organization of

<sup>a)</sup> Authors to whom correspondence should be addressed.

<sup>b)</sup> Tel.: +61-8-8201-2005 (Shapter) or +61-8-8201-5338 (Voelcker); electronic mail: joe.shapter@flinders.edu.au or nico.voelcker@flinders.edu.au

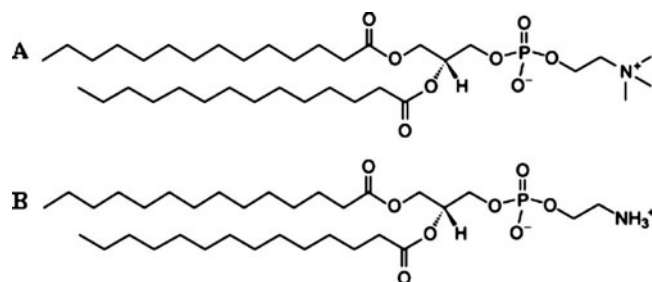


FIG. 1. Molecular structures of (a) dimyristoyl phosphatidylcholine (DMPC) and (b) dimyristoyl phosphatidylethanolamine (DMPE). DMPC and DMPE both comprise a zwitterionic headgroup, each containing a negatively charged phosphate group and either a quaternary or primary amine, respectively.

phospholipids provides insight into how cells maintain their boundaries between different organelles in regard to interorganelle membrane traffic.<sup>8</sup> The phase equilibria of two component lipid bilayers have been investigated both experimentally<sup>10,12–15</sup> and theoretically.<sup>5,7,16,17</sup> In particular, molecular simulations have indicated a random distribution of PE lipids in mixed PC/PE bilayers, with no evidence of PE aggregation.<sup>5,7</sup> The ability to discriminate between either superlattice or domain formation is important for understanding the regulation of membrane lipid compositions.<sup>15</sup>

Scanning probe microscopy, in particular, atomic force microscopy (AFM), has been used to obtain high resolution surface images of biological membranes and meet the resolution requirements to characterize bilayer domains and phases.<sup>2,18–20</sup> Experiments typically employ a supported phospholipid bilayer (SPB) for the characterization of membrane structure,<sup>2,3,21</sup> drug interactions,<sup>1,22–24</sup> and transmembrane protein structure.<sup>25,26</sup> SPBs, as the name implies, are planar, extended bilayers that are adsorbed onto suitable flat substrates, typically mica or silicon, separated from the surface only by a thin layer of water.<sup>27,28</sup> Previous studies have investigated substrate interactions with the lipid headgroups of the lower leaflet. Decoupling occurs in the phase transition between each bilayer leaflet since the solid substrate stabilizes the lipid solid phase.<sup>12,29,30</sup> This was observed as a contrast in topography for temperatures above the transition temperature ( $T_M$ ) phospholipid. The ability of AFM to elucidate the fine structure of membrane surfaces has become particularly useful for understanding how membrane domains influence cellular function.

Previous AFM studies of pure dimyristoyl phosphatidylcholine (DMPC)<sup>31</sup> and DPPE<sup>32</sup> SPBs produced images with an area of  $\leq 400 \text{ nm}^2$ . Under these conditions, regularly spaced ridges on the SPB surface, interpreted as rows of PE molecules, are observed.<sup>31</sup> Studies performed with 1-palmitoyl-2-oleoyl-sn-glycero-3-phosphoethanolamine (POPE) bilayers mixed with cardiolipin have also revealed the existence of three lipid domains, an unanticipated result as only two were expected.<sup>2,33</sup> A mixture of POPE and 1-palmitoyl-2-oleoyl-sn-glycero-3-phosphoglycerol also demonstrated unexpected domain formation.<sup>19</sup> Although the function of these unforeseen do-

main is not entirely clear, Domenech *et al.*<sup>19</sup> speculated that the presence of POPE in membranes gives rise to segregated domains that may be involved in the insertion of proteins.

The current study focuses on the phase behavior and lateral organization of saturated PE and PC bilayers. Since these two lipid headgroups comprise the major fraction of membrane headgroups in eukaryotic cells, a thorough understanding of the bilayer membranes formed from these lipids will help identify their importance in cellular function. In particular, a previous study demonstrated a role for membrane tension in the activity of transmembrane proteins.<sup>34</sup> Experiments were performed here using atomic force microscopy and force-volume (FV) imaging. Utilizing chemically modified AFM probes, the hydrogen bonding capacity of the pure PE and two component (PE/PC) bilayers were also investigated. The results suggest that locations capable of hydrogen bonding to external carboxy-modified AFM probes may be important in the facilitation of membrane protein insertion and chaperone protein activity.

## II. MATERIALS AND METHODS

### A. Vesicle preparation

Multilamellar vesicles were prepared by first dissolving aliquots of DMPE and/or dimyristoyl phosphatidylcholine (DMPC) (Avanti Polar Lipids, Birmingham, AL, USA) in chloroform, followed by evaporation of the solvent under nitrogen. Lipid samples were further dried under vacuum for 3 h prior to being suspended in 10 mM HEPES buffer, 150 mM NaCl pH 9.2 or 7. A pH of 9.2 was necessary to form stable unilamellar DMPE vesicles,<sup>35</sup> otherwise strong attraction between lipid headgroups promotes an inverted hexagonal phase where the hydrocarbon tails face out toward the aqueous medium.<sup>36</sup> Inverted hexagonal phases are an example of nonlamellar phases. The final concentration of lipids was 1 mM. Samples were left to hydrate for 2 h and then sonicated for 30 min with periodic vortex mixing. Vesicle extrusion (Avanti Mini-Extruder, Avanti Polar Lipids, Birmingham, AL, USA) was conducted 20 times (both forward and back) through a polycarbonate membrane filter of defined pore diameter, typically 100 nm. One final extrusion through the membrane ensured that the down stream side of the membrane, where the sample used is taken from, has only vesicles of interest. Extrusion was performed at temperatures above the  $T_m$  phospholipids, since gel-state lipids are difficult to extrude at lower temperatures.<sup>37</sup> Resultant small unilamellar vesicles (SUVs) had a monodisperse size distribution, as measured by dynamic light scattering (HPPS, Malvern Instruments) and were used for all further experiments.

### B. AFM imaging

The visualization of SPBs was performed using a commercial AFM (Nanoscope IV, Digital Instruments, Santa Barbara, CA). All images were obtained by means of *in situ* tapping mode using triangular  $\text{Si}_3\text{N}_4$  cantilevers (Digital Instruments) with a spring constant of  $0.15 \text{ N m}^{-1}$  operating at

the cantilever resonance frequency. Formation of SPBs was achieved by depositing 100  $\mu\text{l}$  of 100 nm SUV solution onto a freshly cleaved mica surface (all SUV solutions were incubated at temperatures greater than their gel-fluid phase  $T_m$  prior to deposition). The prepared surfaces were then incubated for 20–40 min either at 25 °C or above their  $T_m$ . Prior to imaging, surfaces were rinsed with 10 mM HEPES, 150 mM NaCl pH 5.5, pH 7, or pH 9.2 to remove excess vesicles. A Nanoscope heater controller (model: HS-1) was utilized in experiments requiring temperature adjustment. Heating was applied in steps of  $\sim 0.5$ –2 °C, with 5 min for equilibration. Several scans were acquired for each temperature until no noticeable changes in domain structure were observed.

### C. Chemical modification of AFM probes

Commercial  $\text{Si}_3\text{N}_4$  cantilevers functionalized with amine termination were purchased from Novascan (Novascan Technologies, Ames, IA). The surface amine groups were converted to a carboxylic acid functional surface as described elsewhere.<sup>38,39</sup> The amine-terminated cantilever was incubated overnight at 20 °C in a mixture of succinic anhydride 7.5 mg (7.5 mmol) in pyridine (0.5 ml) and 1-methylimidazole:THF (4:21, 0.5 ml) (where THF denotes tetrahydrofuran). The modified cantilever was washed with pyridine (3 ml) and THF (3 ml) and then dried under  $\text{N}_2$ . Subsequently, all unreacted amine groups were capped using a mixture of 1-methylimidazole:THF (4:21, 2 ml) and acetic anhydride:2,6-lutidine:THF (1:1:8, 2 ml). The cantilever was further incubated in this second mixture for 2 h at 20 °C, and then washed with THF (1 ml), pyridine (1 ml), and acetonitrile (3 ml) and dried under  $\text{N}_2$ . Unless stated otherwise, measurements were performed in 10 mM HEPES, 1 mM NaCl, pH 7 for all experiments utilizing carboxylic acid termination.

### D. Force spectroscopy and force-volume imaging

Force plots were acquired using either triangular  $\text{Si}_3\text{N}_4$  cantilevers or modified  $\text{Si}_3\text{N}_4$  cantilevers with nominal spring constants of 0.15 and 0.12  $\text{N m}^{-1}$ , respectively. Spring constants were determined for unmodified and modified probes using the method developed by Sader *et al.*<sup>40</sup> The measured force constants agreed with the manufacturer's nominal values for both the unmodified and modified probes. The quality factor ( $Q$ -factor) of the cantilever for unmodified and modified probes yielded  $Q \sim 61$  and 56, respectively.

FV images ( $32 \times 32$  force curves) were collected at a scan rate of 0.0962 Hz, in relative trigger mode. The trigger mechanism was set to 125 nm of cantilever deflection. The force measurements presented are given with  $\pm$  one standard deviation. These values are accompanied by the total number ( $n$ ) of force measurements analyzed for each experiment.

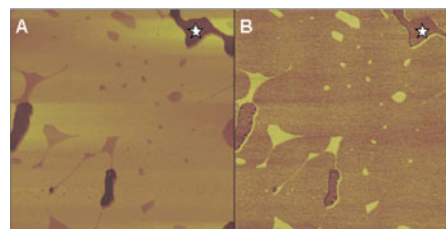


FIG. 2. (A) AFM topographic image ( $5 \times 5 \mu\text{m}^2$ ; Z-scale: 10 nm, 512 lines  $\times$  512 lines) and (B) phase (Z-scale:  $10^\circ$ ) of a DMPE supported phospholipid bilayer (pH 9.2). UD extend  $0.97 \pm 0.04$  nm above surrounding LD. Phase shift measured between the UD and LD was  $\sim 2.5^\circ$ . The white stars correspond to the mica substrate.

## III. RESULTS AND DISCUSSION

### A. Pure DMPE bilayers

Initial experiments investigated the surface topology of SPBs formed by DMPE vesicles at room temperature [Fig. 2(A)]. Since the  $T_m$  of DMPE is  $\sim 50$  °C, only solid phase should be observed at room temperature. Results demonstrated the existence of two membrane heights. The upper domain (UD), with a height of  $4.74 \pm 0.26$  nm (measured from defects), was  $0.97 \pm 0.20$  nm higher than the lower domain (LD). In the case of single component SPBs, height differences of this magnitude are typically assigned to different lipid lamellar phases. Phase imaging was employed to provide further insight into the two observed membrane heights. The phase lag of the tip relative to the excitation signal is sensitive to surface properties, such as adhesion and viscoelasticity. Phase imaging revealed a strong phase difference between the UD and the LD [Fig. 2(B)]. This contrast was interpreted as a change in bilayer compactness.<sup>41,42</sup> Examining the phase shift between the hard mica surface, and the UD and LD, respectively, a smaller contrast was observed for the UD, suggesting that the LD is less compact and softer than the UD.

Because incubation conditions can affect bilayer formation, DMPE liposomes were also incubated at 10 °C above their  $T_m$  to investigate the effects on bilayer structure. Although the existence of two membrane lamellar phases was still present, the ratio of LD to UD increased from 0.1 to 0.89 (Fig. 3).

The  $pK_a$  of the amine functionality of the DMPE head-group is approximately 11.<sup>43</sup> Previous research, however, has demonstrated surface bound amine groups exhibit a  $pK_a$  of about 5.<sup>44</sup> Experiments thus far had been carried out at pH 9.2, but since experiments performed at pH 7 did not demonstrate any noticeable change in surface topology (data not shown), further work was performed at pH 7 in order provide a closer physiological mimic. The lateral heterogeneity of the samples was characterized by obtaining force-extension curves from which nanomechanical properties of each membrane domain were determined. Force-extension curves can provide useful information regarding the maximum force that a membrane can withstand before breaking.<sup>45–47</sup> FV imaging collects force curves at each  $x, y$  pixel of the image by measuring cantilever deflection. While

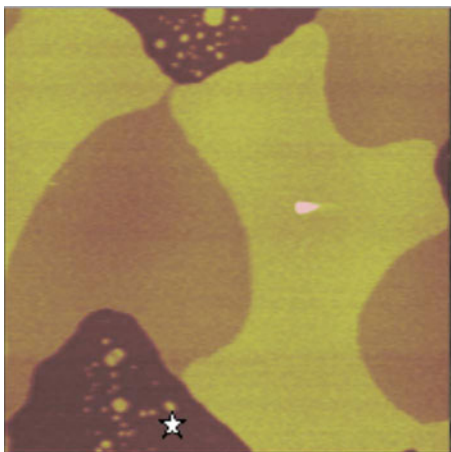


FIG. 3. AFM topographic image ( $3.0 \times 3.0 \mu\text{m}^2$ ; Z-scale: 10 nm, 512 lines  $\times$  512 lines) of a DMPE supported phospholipid bilayer that was heated above its  $T_m$  during incubation (pH 9.2). The white star corresponds to the mica substrate.

a height image is also produced, the strength of this technique is that the information contained in the three-dimensional data set can be decoupled from the topographic information. This information can then be employed to assist in identifying the lamellar phase of a particular membrane domain, as greater force is required to breakthrough the gel phase than the liquid phase. With respect to the measured

force-extension curves, FV imaging demonstrated the existence of two different lamellar phase domains on the bilayer membrane [Fig. 4(B)]. Figure 4(A) is the high resolution tapping mode image acquired in the exact same location as Fig. 4(B). As observed in Fig. 2, the differences in height allow identification of locations corresponding to the UD and LD. Force curves obtained at room temperature ( $\sim 22^\circ\text{C}$ ) demonstrated a jump-to-contact in the approach curve for locations in the UD and LD, corresponding to breakthrough forces of  $2.02 \pm 0.42 \text{ nN}$  ( $n=100$ ) and  $0.10 \pm 0.27 \text{ nN}$  ( $100 \pm 27 \text{ pN}$ ) ( $n=100$ ), respectively [Fig. 4(C)]. Previous studies of POPE bilayer membranes in their gel state have reported similar yield threshold values to those obtained here for the UD here.<sup>48</sup> Measurements performed on POPE monolayers in the liquid-condensed phase have also demonstrated breakthrough forces of 1.72 nN. However studies with POPE monolayers in their liquid-expanded phase were not capable of detecting a breakthrough force. This was attributed to the low mechanical resistance of the POPE monolayer, making it impossible to detect the jump to contact in an AFM experiment.<sup>45</sup> We believe that the POPE monolayer in the liquid-expanded state exhibits similar mechanical properties to that observed in the current study for the LD. In general, there are conspicuous differences in the mechanical stability between the UD and LD, the LD being the less stable domain. On the other hand, the force curves for UD and LD demonstrated equivalent forces of adhesion, typically

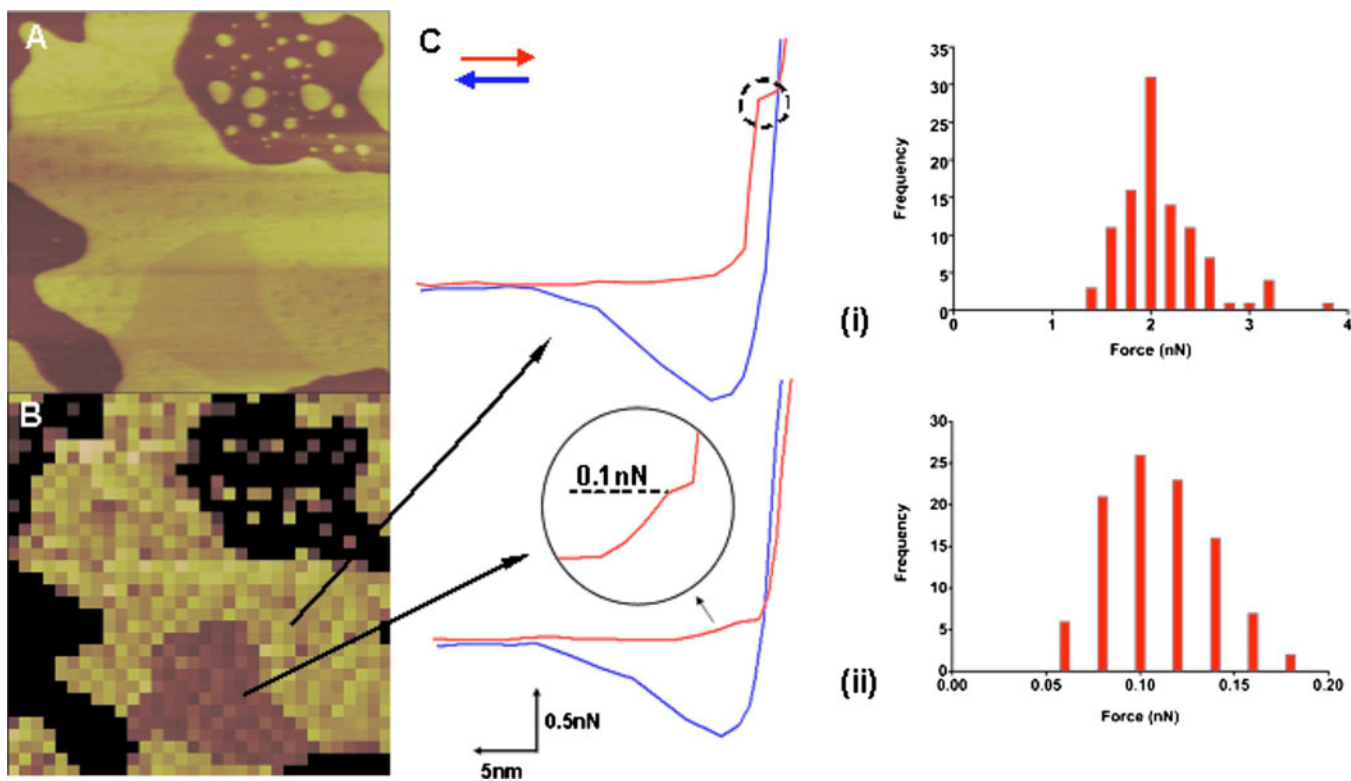


FIG. 4. (A) AFM height image ( $2.0 \times 2.0 \mu\text{m}^2$ , Z-scale: 10 nm, 512 lines  $\times$  512 lines) of a DMPE supported phospholipid bilayer. (B) FV map ( $2.0 \times 2.0 \mu\text{m}^2$  Z-scale: 10 nm, FV scale: 5 nm, 32<sup>2</sup> force curves) performed in the exact same location with its associated (c) force curves for both the (i) UD and (ii) LD. A breakthrough force (circled region on force curves) equivalent to  $2.02 \pm 0.42 \text{ nN}$  (i) and  $100 \pm 27 \text{ pN}$  (ii) was observed at the UD and LD regions, respectively. Statics of breakthrough force measurements for the (i) UD and (ii) LD are also presented. UD and LD demonstrated forces of adhesion, typically  $\sim 0.9 \text{ nN}$ . Standard  $\text{Si}_3\text{N}_4$  probes were utilized. Measurements were performed in 10 mM HEPES, 150 mM NaCl, pH 7.

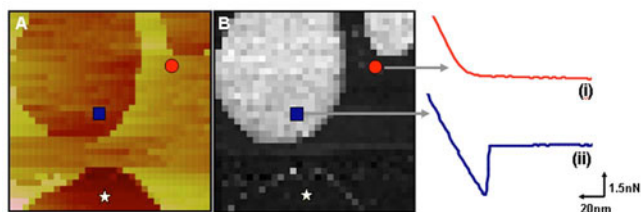


FIG. 5. (A) AFM height image ( $1.1 \times 1.1 \mu\text{m}^2$ , Z-scale: 10 nm,  $32 \text{ lines} \times 32 \text{ lines}$ ). (B) FV adhesion map ( $1.1 \times 1.1 \mu\text{m}^2$ ,  $32^2$  forces curves) of a DMPE supported phospholipid bilayer. Lighter regions in the FV adhesion map correspond to greater adhesion force associated with the LD (blue squares). Both UD (red circles) and mica substrate ( $\star$ ) measured no adhesion. The numbers (i) and (ii) label the corresponding force curves for the UD and LD, respectively. Histogram of adhesive forces measured for the LD at  $p\text{H } 7$  is available in the supplementary material (see Ref. 59). All measurements were performed in 10 mM HEPES 1 mM NaCl  $p\text{H } 7$  with a carboxy-modified tip.

$\sim 0.9$  nN, for both membrane domains [Fig. 4(C)]. Since the maximum force applied is above the breakthrough force for both bilayer domains, the tip is in contact with the mica surface prior to the retract cycle. Subsequent retraction of the tip then demonstrates equivalent forces of adhesion as the molecular properties of each domain are identical.

Further studies utilized a carboxy-modified probe to increase interactions with the primary amine located at the headgroup of DMPE. Since PE hydrogen bonds with itself and neighboring lipids in a bilayer,<sup>5</sup> it was assumed that a modified probe would be able to interact with regions that were available for hydrogen bonding. Experiments were also performed in a 10 mM HEPES 1 mM NaCl  $p\text{H } 7$  (low salt buffer) in order to reduce the high electrostatic double-layer contribution, thus exposing the tip to short range forces with the DMPE bilayer. As previous measurements with an unmodified probe demonstrated equivalent adhesive forces for both locations in the pure DMPE bilayer [Fig. 4(C)], a trigger threshold above the breakthrough force of both bilayer domains was also employed in the modified tip experiments. We believe these measurement conditions were the most suitable for providing a reliable contrast for the modified probe, as performing measurements below the breakthrough force for both bilayer domains, particularly the LD (where the breakthrough force is 100 pN), would have been extremely difficult in low salt buffer.

Force retraction curves were used to acquire information related to the adhesion of the probe with the sample surface. In association with these force retraction curves, Fig. 5 presents a FV image, together with a  $32 \times 32$  pixel resolution topographic contact mode image of a DMPE bilayer measured in low salt buffer. Compared to previous images measured with  $\text{Si}_3\text{N}_4$  tips and higher salt concentration, cross-sectional analysis (data not shown) of the topographic image from defect locations shows a further decrease in the height of the LD ( $3.30 \pm 0.12$  nm). However, the height of the UD ( $4.90 \pm 0.10$  nm) remained unaffected. We speculate that removal of the high electrostatic double-layer decreases the mechanical resistance of the phospholipid bilayer,<sup>48</sup> making it difficult to prevent the modified tip from partially indent-

ing the LD surface. Previous work also demonstrated the ability of the AFM tip to easily penetrate and partially deform liquid phase domains of POPE<sup>45</sup> and DOPE monolayers.<sup>49–51</sup> With respect to the measured forces, large adhesion ( $2.85 \pm 0.28$  nN,  $n=450$ ) was observed for the LD of the DMPE bilayer [Fig. 5(B)(i)], but no adhesion was observed for the UD [Fig. 5(B)(ii)]. This resulted in a highly contrasted adhesion FV image. It is also important to note that no adhesion was observed for the interaction with the mica substrate (Fig. 5), thus confirming that the observed adhesion is indeed due to interactions of the AFM tip with the lipids in the LD. In agreement with previous work,<sup>49</sup> we attribute the absence of adhesion on the UD to higher mechanical stability (refer to Fig. 4) that is indicative of strong lateral interactions between phospholipid molecules. This cohesive force between the phospholipid molecules resulting from lipid amine and phosphate group hydrogen bonding prevents the carboxy-modified tip from hydrogen bonding with the amine group of DMPE. The LD of the DMPE bilayer, however, represents locations of low mechanical stability, typically yielding adhesion forces of  $\sim 2.9$  nN. The detection of adhesion on these locations may be attributed to hydrogen bonding between the carboxylic acid terminated tip and the N-terminus of the DMPE bilayer headgroup.

Experiments were conducted at  $p\text{H } 5.5$  to further investigate the interactions between the LD and the carboxy-modified tip. The measured adhesion on the UD remained unchanged; however an increase in adhesion for the LD was observed ( $12.18 \pm 0.51$  nN,  $n=200$ ) compared to  $p\text{H } 7$  (2.85 nN). The UD's have a very high breakthrough force which must be due to extensive lipid-lipid interactions. These strong interactions are very likely to be due to hydrogen bonding and will make the packing in these regions quite tight. This will lead to a rigid structure where many of the groups that might be affected by changes in  $p\text{H}$  are not readily available to react and hence the properties of these regions will not change. On the other hand, for the LD areas there is a very low breakthrough force implying a loose packing which will of course mean that the bilayer can react with the hydrogen ions available and this will change the properties of these regions.

Previous results for the interaction between carboxylic acid functionalized AFM tips and poly(allylamine) surfaces have also demonstrated an increase in adhesion at  $p\text{H} < 7$ .<sup>52</sup> A previous study reported maximum adhesion force at  $p\text{H } 4$ , which was believed to represent a large interaction between uncharged carboxy groups of the AFM tip and uncharged amines of the poly(allylamine) surface.<sup>52</sup> Studies investigating the interaction between amine modified tips and self-assembled monolayers of carboxy-functionalized thiols have demonstrated peak interactions around  $p\text{H } 7$ , however, literature values for acid-base interactions vary substantially depending on the system being investigated.<sup>44</sup> Comparable interactions are at play in the current study between the carboxy-modified tip and the surface amines of the DMPE bilayer surface. The magnitude of this interaction was also confirmed by the AFM tip partially indenting the LD while

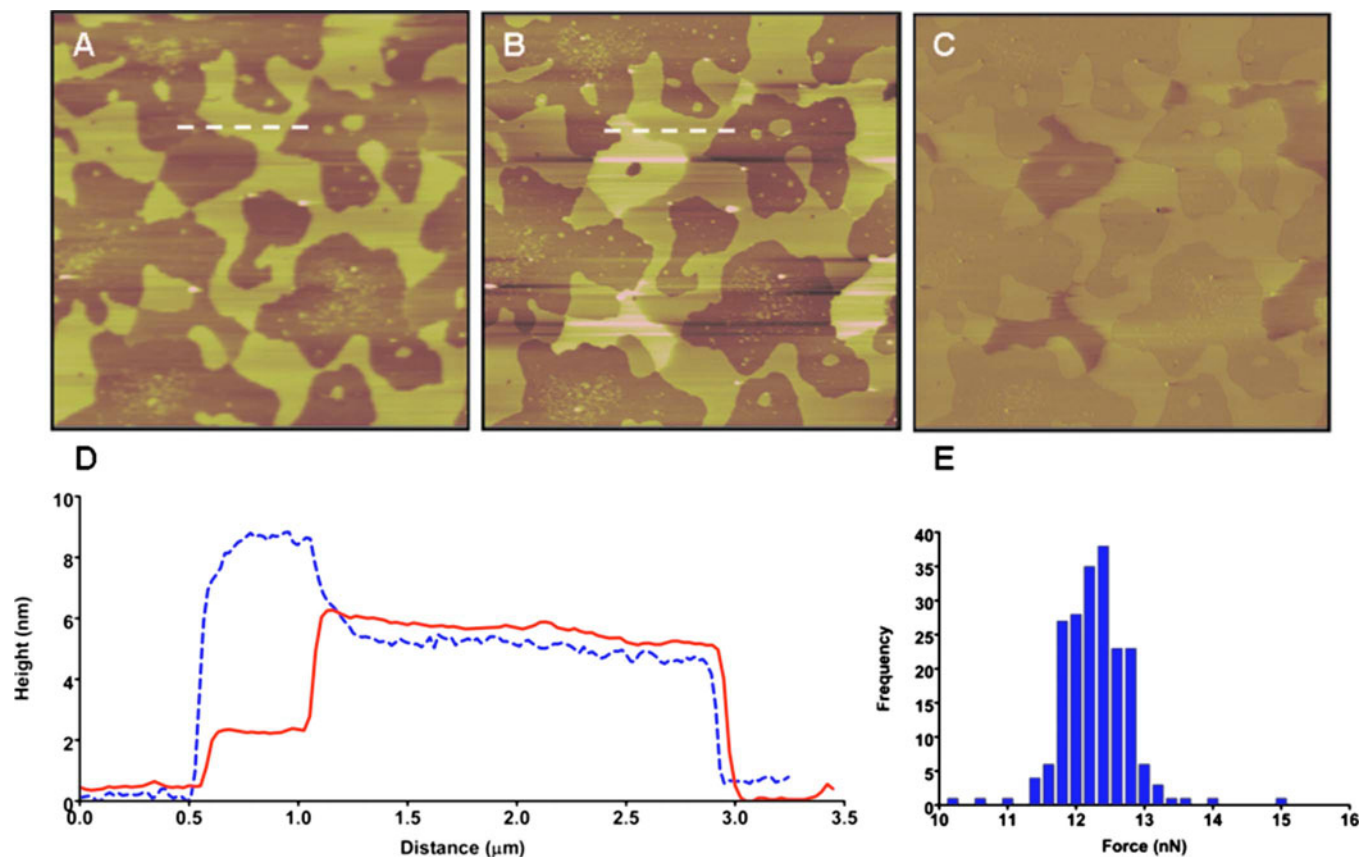


FIG. 6. (A) Contact mode AFM height image ( $10.0 \times 10.0 \mu\text{m}^2$ , Z-scale: 20 nm, 256 lines  $\times$  256 lines) of a DMPE supported phospholipid bilayer. (B) High resolution topographic tapping mode height image ( $10.0 \times 10.0 \mu\text{m}^2$ , Z-scale: 20 nm, 512 lines  $\times$  512 lines) and (C) phase image (Z-scale:  $50^\circ$ ). All images were collected in the exact same location. (d) Cross-section analysis performed at marked locations of contact (—) and tapping (---) mode topographic images. All measurements were performed in 10 mM HEPES 1 mM NaCl pH 5.5 with a carboxy-modified tip. (e) Histogram of adhesive forces measured for the LD at pH 5.5. All measurements were performed in 10 mM HEPES 1 mM NaCl pH 5.5 with a carboxy-modified tip.

imaging in contact mode. The typical height observed for the LD was  $1.83 \pm 0.48 \text{ nm}$  [Figs. 6(A) and 6(D)], significantly lower than previously observed at pH 7. The height of the UD, however, was  $4.96 \pm 0.29 \text{ nm}$ , comparable to previous measurements. The location of LDs was also confirmed by collecting images in high salt buffer for the same surface, where a domain height of  $3.46 \pm 0.19 \text{ nm}$  was measured. This was in good agreement with measurements performed at pH 7.

Interestingly experiments performed in tapping mode under low salt buffer (pH 5.5) demonstrated an extensive height increase for the LD. The new measured height was typically  $7.91 \pm 0.45 \text{ nm}$  [Figs. 6(B) and 6(D)]. This was accompanied by a very large phase shift ( $\sim 7.4^\circ$ ) between the UD and LD [Fig. 6(C)]. Under other conditions with  $\text{Si}_3\text{N}_4$  AFM tips, a phase shift of  $\sim 2.5^\circ$  or less between the UD and LD was always observed. In contrast, however, the current experiment was performed at pH 5.5 (low salt buffer) with a carboxy-modified tip and large adhesions on the LD were observed [Fig. 6(E)].

We believe this unanticipated result regarding the substantial height variation is related to an artifact of tapping mode AFM imaging. In a study investigating vacancy sites between close-packed polystyrene colloids,<sup>53</sup> Dinte *et al.* re-

ported an artifact which may be relevant to the present work. Using tapping mode AFM, a “ghost” sphere of regular structure and height was observed in the vacancy sites of a colloidal layer. The absence of a colloidal sphere at these locations was confirmed using contact mode AFM. The ghost feature was thought to arise from the capillary forces present in ambient conditions due to the presence of water. In particular, the capillary forces located in the vacancy site of a colloidal layer effectively localize a strong interaction between the tip and surface, acting much like a rubber band and damping the oscillation amplitude of the cantilever. To maintain the operating set point, the AFM stage then adjusts position forming the ghost sphere image. We believe a similar process is occurring between our carboxy-modified AFM tip and the LD of the lipid bilayer. The strong adhesive interaction [confirmed by force curve analysis, Fig. 6(E)] of the LD of the DMPE bilayer with the carboxy-modified tip forms a “bridge” between the tip and surface, much like the capillary forces in the study of Dinte *et al.* This adhesive force damps the amplitude of the tip causing an apparent increase in the height of the LD. As previously discussed, however, contact mode images showed a decrease in the thickness of the lipid layer [refer to Figs. 6(A) and 6(D)]. This is not surprising since the adhesion between tip and surface in contact mode

will contribute to the total imaging force. Thus, greater force is applied to this region of the surface which causes the tip to partially indent the LD in contact mode. In general, the artifact we observed in tapping mode AFM suggests a very large interaction with our carboxy-modified AFM tip and the surface amines of DMPE (also confirmed by phase imaging). This interaction is not unexpected and likely due to hydrogen bonding.

Although saturated phospholipids are less abundant than unsaturated lipids in physiological membranes, the LD observed in DMPE bilayers could nevertheless occur in natural membranes. In this regard, it is known that the presence of PE phospholipids is essential for the binding and function of peripheral and integral membrane proteins, respectively.<sup>45,54</sup> The results from the current study demonstrate the ability of DMPE based membranes to exert different lateral pressures among lipid headgroups, an effect that is exploited in the process of protein insertion.<sup>54</sup> Previous studies utilizing POPE also reported unexpected segregated domains, and it was proposed that these regions may play a role in protein insertion.<sup>19</sup> There is evidence suggesting that the ability of phospholipids to form hydrogen bond is relevant to the activity of transmembrane proteins.<sup>2,55,56</sup> An example of the importance of protein-lipid interactions is<sup>45</sup> the mechanosensitive high conductance channel of *Mycobacterium tuberculosis*, which is gated by membrane tension, and is fully functional when reconstituted alone into lipid vesicles.<sup>34</sup> Molecular dynamics simulations further demonstrated the ability of this protein to extensively hydrogen bond to PE phospholipid headgroups, and differences in hydrogen bonding patterns between lipid environments were apparently related to differences in gating tension of the channel.<sup>55</sup> The results from the current study revealed that the less laterally condensed locations were potentially available for hydrogen bonding, since adhesion was observed between the tip and the amine groups of the DMPE bilayer. Thus, a role for these lower domains in membrane protein insertion and activity seems plausible.

## B. Binary phospholipid bilayers: DMPC and DMPE

Biological membranes comprise many phospholipids, emphasizing the need to investigate the phase behavior arising from even slight differences in chemical structure. Hence the mixing behavior of PE and PC was studied since these phospholipids are the major constituents of most mammalian cell membranes. Although previous work has demonstrated the phase equilibria for freestanding DMPC/DMPE bilayers utilizing two-photon fluorescence microscopy,<sup>14</sup> the analysis of this system as a supported bilayer by AFM has not yet been performed. In addition to high resolution imaging, FV imaging was employed to provide insights into the mixing properties of these two lipids.

Binary mixtures of DMPC and DMPE were prepared in a 1:1 ratio. AFM topology and phase images at room temperature revealed a phase separated phospholipid bilayer. Gel domains and liquid domains on the upper leaflet were confirmed by phase imaging, as there was a large phase dif-

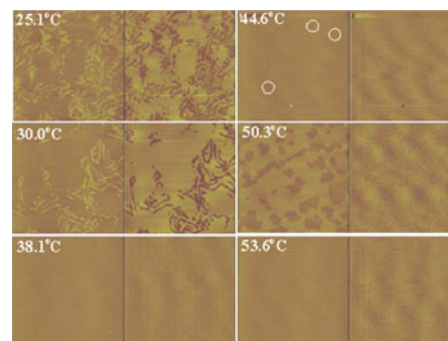


FIG. 7. (A) Temperature dependent tapping mode AFM height images ( $4.0 \times 4.0 \mu\text{m}^2$ ; Z-scale: 5 nm, 512 lines  $\times$  512 lines) and (B) phase (Z-scale: 5°) images of a binary mixture of DMPC:DMPE (1:1). Temperatures are as indicated. All measurements were performed in 10 mM HEPES 150 mM NaCl pH 7. Complete set of data available in the Supplementary Material (Ref. 59).

ference between the two different locations on the bilayer surface [Fig. 7(B), 25.1 °C]. Gel domains were  $0.649 \pm 0.030$  nm higher than the neighboring liquid phase domains (Fig. 7, 25.1 °C). Changes in topography and phase as a function of temperature were also measured (Fig. 7, 25.1–53.6 °C). Increasing the temperature resulted in melting of the gel domains of the upper leaflet, such that at 38.1 °C the entire upper leaflet was in the liquid phase. Consistent with previous studies, further temperature increases initiated the melting of the lower leaflet, as demonstrated by the circled location in Fig. 7 (44.6 °C). Melting of the lower leaflet occurred at 53.6 °C, converting the entire bilayer to the liquid phase. Interestingly, DMPC and DMPE have very different  $T_m$  values, 21 and 50 °C, respectively. However the bilayer mixture did not demonstrate monotectic behavior, consistent with previous measurements performed on DPPC/DPPE bilayers.<sup>57</sup> Differential scanning calorimetry has also demonstrated only a single endothermic peak for mixtures of PC and PE, provided the PE content is above 50%.<sup>58</sup> In addition, the endothermic peak varied with composition, such that an increase in PE content shifted the peak to higher temperatures. Two-photon fluorescence data for freestanding DMPC/DMPE<sup>14</sup> and DPPC/DPPE bilayers<sup>10</sup> demonstrated similar trends, such that a single melting event for the solid-to-fluid state transition was observed. In addition, the phase transition temperature for these bilayers was dependent on their composition. Temperature dependency studies for a 1:4 mixture of DMPC:DMPE were also performed in the current study and, as predicted, an increase in the  $T_m$  was observed (data not shown). The upper leaflet was completely melted at 42.8 °C. A  $T_m$  for the lower leaflet was not observed, as the temperature controller could only heat to a maximum of 60 °C.

Utilizing FV imaging and a carboxylic acid functionalized AFM probe, the lateral organization of a 1:1 DMPC:DMPE bilayer mixture in low salt buffer (pH 7) was investigated. Measurements for the FV experiments were additionally performed above the breakthrough force of both component phospholipids. Figure 8 shows a high resolution image (A),

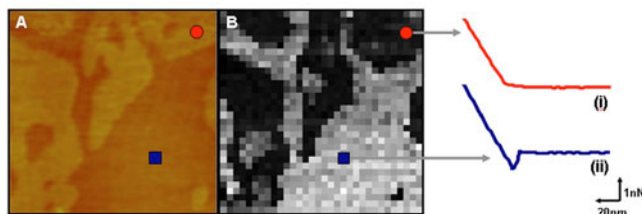


FIG. 8. (A) High resolution contact mode AFM height image ( $1.1 \times 1.1 \mu\text{m}^2$ , Z-scale: 10 nm, 512 lines  $\times$  512 lines). (B) FV adhesion map ( $32^2$  forces curves) of a DMPC:DMPE 1:1 supported phospholipid bilayer. Lighter regions in the FV adhesion map correspond to greater force associated with the LD (blue squares). The numbers (i) and (ii) label the corresponding force curves for the UD (red circles) and LD (blue squares), respectively. Histogram of adhesive forces measured for the LD is available in the supplementary material (see Ref. 59). All measurements were performed in 10 mM HEPES 1 mM NaCl pH7 with a carboxy-modified tip.

together with an adhesion FV image (B) captured at the same location. Force retraction curves demonstrated the existence of two regions; one presenting no adhesion [Fig. 8(B)(i)] and the other showing small signs of interaction [Fig. 8(B)(ii)]. Measurements performed on pure DMPC bilayers, for both liquid and gel phase domains, demonstrated no adhesion to the modified probe (data not shown). In contrast to previous DMPE results, the height difference between the UD and LD observed for the mixed bilayer at high and low salt concentrations did not change substantially. This is indicative of high mechanical stability for the entire mixed bilayer. Moreover, the adhesion measured at the LD was  $1.82 \pm 0.52$  nN ( $n=450$ ), about half that observed for DMPE alone. As the liquid phase domains for pure DMPC do not adhere to the modified probe, it can be assumed that DMPE is responsible for the adhesion observed at these lower locations. Assuming that PE acts as a spacer, essentially relieving the repulsion between bulky PC headgroups,<sup>7</sup> it seems reasonable that lower adhesion occurs for LDs of the binary mixture in comparison to those of the pure DMPE bilayer, as the overall interaction would result from the contribution of both DMPC and DMPE lipids in their liquid phase. The UD of this binary mixture provided retraction curves without an adhesive component, similar to those observed for the gel domains in pure DMPE bilayers. Together with the observation of a single melting transition at each bilayer leaflet, and the fact that melting of gel domains in binary mixtures of DMPE/DMPC was dependent on relative composition of each phospholipid component, it is clear that these domains are in fact comprised of both lipids.

### C. Summary and conclusions

AFM was used to investigate the structural properties of single component supported DMPE bilayers and binary mixtures comprising DMPE and DMPC. The results for pure DMPE bilayers revealed unexpected domain formation. In particular, domains that were less stable and had the ability to hydrogen bond to carboxylic acid groups were observed (LDs). At high ionic strength, breakthrough forces of around  $\sim 2$  nN were observed for UD, and these regions showed

no adhesion to modified carboxylic acid terminated probes. We postulate that the UD phospholipids form a highly ordered hydrogen bonded network and thus they are robust and resist mechanical deformation due to a restricted ability to hydrogen bond to external carboxylic acids. The LDs, however, are softer (breakthrough force equivalent to  $\sim 100$  pN) and less ordered, and thus potentially could facilitate protein binding through intermolecular hydrogen bonding at the protein-membrane interface. The mixing behavior of DMPE with DMPC phospholipids was also investigated. Temperature dependence AFM studies demonstrated the phase transition temperature of these mixed PC/PE bilayers was dependent on composition. These two lipids differ only by their substituents at the N-terminus of the headgroup. However, the ability of DMPE to form intermolecular hydrogen bonds to neighboring PC and PE headgroups increased (depending on relative concentration) the  $T_m$  of the mixed PC:PE bilayer systems substantially. Together with information acquired by FV imaging, the work presented in this study demonstrates the ability of these two lipids to intermix and hydrogen bond.

AFM, together with FV imaging, has been demonstrated to be a useful technique in the characterization of single and binary component bilayer membranes. The current work furthers our understanding of the mixing behavior of PE and PC phospholipids. Future studies will combine a diverse range of phospholipid bilayer mixtures, together with additional probe functionalities, in order to further characterize and understand membrane structure and function.

### ACKNOWLEDGMENTS

This work was supported by the Australian Microscopy and Microanalysis Research Facility (AMMRF). The authors wish to thank Mickey Huson and co-workers from CSIRO (Textile and Fiber Technology) for providing and offering assistance with the software "FORCE VOLUME."

- <sup>1</sup>M. R. Nussio, M. Liddell, M. J. Sykes, J. O. Miners, and J. G. Shapter, *J. Scanning Probe Microsc.* **2**, 41 (2007).
- <sup>2</sup>O. Domenech, F. Sanz, M. T. Montero, and J. Hernandez-Borell, *Biochim. Biophys. Acta* **1758**, 213 (2006).
- <sup>3</sup>S. Chiantia, J. Ries, N. Kahya, and P. Schwille, *ChemPhysChem* **7**, 2409 (2006).
- <sup>4</sup>M. L. Kraft, P. K. Weber, M. L. Longo, I. D. Hutcheon, and S. G. Boxer, *Science* **313**, 1948 (2006).
- <sup>5</sup>S. Leekumjorn and A. K. Sum, *Biophys. J.* **90**, 3951 (2006).
- <sup>6</sup>M. Kranenburg and B. Smit, *J. Phys. Chem. B* **109**, 6553 (2005).
- <sup>7</sup>A. H. de Vries, A. E. Mark, and S. J. Marrink, *J. Phys. Chem. B* **108**, 2454 (2004).
- <sup>8</sup>P. Somerharju, J. A. Virtanen, and K. Hon Cheng, *Biochim. Biophys. Acta* **1440**, 32 (1999).
- <sup>9</sup>K. Hon Cheng, M. Ruonala, J. Virtanen, and P. Somerharju, *Biophys. J.* **73**, 1967 (1997).
- <sup>10</sup>L. A. Bagatolli and E. Gratton, *Biophys. J.* **78**, 290 (2000).
- <sup>11</sup>T. Ahn and C.-H. Yun, *Biophys. J.* **369**, 288 (1999).
- <sup>12</sup>D. Keller, N. B. Larsen, I. M. Moller, and O. G. Mouritsen, *Phys. Rev. Lett.* **94**, 025701 (2005).
- <sup>13</sup>Z. V. Leonenko, E. Finot, H. Ma, T. E. S. Dahms, and D. T. Cramb, *Biophys. J.* **86**, 3783 (2004).
- <sup>14</sup>L. A. Bagatolli and E. Gratton, *Biophys. J.* **79**, 434 (2000).
- <sup>15</sup>J. A. Virtanen, M. Ruonala, M. Vauhkonon, and P. Somerharju, *Biochemistry* **34**, 11568 (1995).
- <sup>16</sup>B. Y. Wong and R. Faller, *Biochim. Biophys. Acta* **1768**, 620 (2007).
- <sup>17</sup>S. Leekumjorn and A. K. Sum, *Biochim. Biophys. Acta* **1768**, 354

- (2007).
- <sup>18</sup>M. R. Nussio, N. H. Voelcker, B. S. Flavel, C. T. Gibson, M. J. Sykes, J. O. Miners, and J. G. Shapter (unpublished).
- <sup>19</sup>O. Domenech, S. Merino-Montero, M. T. Montero, and J. Hernandez-Borrell, *Colloids Surf.* **47**, 102 (2006).
- <sup>20</sup>I. Reviakine, A. Simon, and A. Brisson, *Langmuir* **16**, 1473 (2000).
- <sup>21</sup>O. Domenech, A. Morros, M. E. Cabanas, M. T. Montero, and J. Hernandez-Borrell, *Biochim. Biophys. Acta* **1768**, 100 (2007).
- <sup>22</sup>A. Berquand, M. P. Mingeot-Leclercq, and Y. F. Dufrene, *Biochim. Biophys. Acta* **1664**, 198 (2004).
- <sup>23</sup>M. T. Montero, M. Pijoan, S. Merino-Montero, T. Vinuesa, and J. Hernandez-Borrell, *Langmuir* **22**, 7574 (2006).
- <sup>24</sup>Z. Leonenko, E. Finot, and D. Cramb, *Biochim. Biophys. Acta* **1758**, 487 (2006).
- <sup>25</sup>S. Merino-Montero, O. Domenech, M. T. Montero, and J. Hernandez-Borrell, *Biophys. Chem.* **119**, 78 (2006).
- <sup>26</sup>H. Mueller, H. Butt, and E. Bamberg, *J. Phys. Chem. B* **104**, 4552 (2000).
- <sup>27</sup>E. Reimhult, F. Hook, and B. Kasemo, *Langmuir* **19**, 1681 (2003).
- <sup>28</sup>E. Sackmann, *Science* **271**, 43 (1996).
- <sup>29</sup>Z. V. Feng, T. A. Spurlin, and A. A. Gewirth, *Biophys. J.* **88**, 2154 (2005).
- <sup>30</sup>S. Garcia-Manyes, G. Oncins, and F. Sanz, *Biophys. J.* **89**, 4261 (2005).
- <sup>31</sup>J. A. N. Zasadzinski, C. A. Helm, M. L. Longo, A. L. Weisenhorn, S. A. C. Gould, and P. K. Hansma, *Biophys. J.* **59**, 755 (1991).
- <sup>32</sup>S. W. Hui, R. Viswanathan, J. A. Zasadzinski, and J. N. Israelachvili, *Biophys. J.* **68**, 171 (1995).
- <sup>33</sup>O. Domenech, A. Morros, M. E. Cabanas, M. T. Montero, and J. Hernandez-Borrell, *Ultramicroscopy* **107**, 943 (2007).
- <sup>34</sup>C. C. Häse, A. C. Le Dain, and B. Martinac, *J. Biol. Chem.* **270**, 18329 (1995).
- <sup>35</sup>J. G. Stollery and W. J. Vail, *Biochim. Biophys. Acta* **471**, 372 (1977).
- <sup>36</sup>J. M. Seddon, *Biochim. Biophys. Acta* **1031**, 1 (1990).
- <sup>37</sup>R. C. MacDonald, R. I. MacDonals, B. P. Menco, K. Takeshita, N. K. Subbarao, and L. R. Hu, *Biochim. Biophys. Acta* **1061**, 297 (1991).
- <sup>38</sup>S. J. P. McInnes, S. D. Graney, Y.-L. Khung, and N. Voelcker, *Proc. SPIE* **6036**, 1 (2007).
- <sup>39</sup>A. Azhayeve and M. Antopolsky, *Tetrahedron* **57**, 4977 (2001).
- <sup>40</sup>J. E. Sader, I. Larson, P. Mulvaney, and L. R. White, *Rev. Sci. Instrum.* **66**, 3789 (1995).
- <sup>41</sup>Z. V. Leonenko, A. Carnini, and D. T. Cramb, *Biochim. Biophys. Acta* **1509**, 131 (2000).
- <sup>42</sup>K. O. Evans, *Int. J. Mol. Sci.* **9**, 498 (2008).
- <sup>43</sup>G. Cevc, A. Watts, and D. Marsh, *Biochemistry* **20**, 4955 (1981).
- <sup>44</sup>M. Giesbers, J. M. Kleijn, and M. A. Cohen Stuart, *J. Colloid Interface Sci.* **252**, 138 (2002).
- <sup>45</sup>S. Garcia-Manyes, O. Domenech, F. Sanz, M. T. Montero, and J. Hernandez-Borrell, *Biochim. Biophys. Acta* **1768**, 1190 (2007).
- <sup>46</sup>S. Garcia-Manyes, P. Gorostiza, and F. Sanz, *Anal. Chem.* **78**, 61 (2006).
- <sup>47</sup>G. Oncins, S. Garcia-Manyes, and F. Sanz, *Langmuir* **21**, 7373 (2005).
- <sup>48</sup>S. Garcia-Manyes, G. Oncins, and F. Sanz, *Biophys. J.* **89**, 1812 (2005).
- <sup>49</sup>Y. F. Dufrêne, W. R. Barger, J. D. Green, and G. U. Lee, *Langmuir* **13**, 4779 (1997).
- <sup>50</sup>Y. F. Dufrêne, T. Boland, J. W. Schneider, W. R. Barger, and G. U. Lee, *Faraday Discuss.* **111**, 79 (1999).
- <sup>51</sup>Y. F. Dufrêne and G. U. Lee, *Biochim. Biophys. Acta* **1509**, 14 (2000).
- <sup>52</sup>A. Valsesia, M. M. Silvan, G. Ceccone, D. Gilliland, P. Colpo, and F. Rossi, *Plasma Processes Polym.* **2**, 334 (2005).
- <sup>53</sup>B. P. Dinte, G. S. Watson, J. F. Dobson, and S. Myhra, *Ultramicroscopy* **63**, 115 (1996).
- <sup>54</sup>E. van den Brink-van del Laan, J. A. Killian, and B. de Kruijff, *Biochim. Biophys. Acta* **166**, 275 (2004).
- <sup>55</sup>D. E. Elmore and D. A. Dougherty, *Biophys. J.* **81**, 1345 (2001).
- <sup>56</sup>A. G. Lee, *Biochim. Biophys. Acta* **1666**, 62 (2004).
- <sup>57</sup>A. Blume, R. J. Wittebort, S. K. Das Gupta, and R. G. Griffin, *Biochemistry* **21**, 6243 (1982).
- <sup>58</sup>T. Inoue and Y. Nibu, *Chem. Phys. Lipids* **100**, 139 (1999).
- <sup>59</sup>See EPAPS Document No. E-BJIOBN-3-001804 for a complete data set for temperature dependent studies for DMPE:DMPC binary supported bilayers. Histograms of adhesive forces measured for carboxy-modified AFM tips and the LDs of pure and binary DMPE phospholipid bilayers are also presented. For more information on EPAPS, see <http://www.aip.org/pubservs/epaps.html>